

Anomalous Nernst effects in pyrochlore molybdates with spin chirality

N. Hanasaki, K. Sano, Y. Onose, T. Ohtsuka, S. Iguchi, István Kézsmárki, S. Miyasaka, S. Onoda, N. Nagaosa, Y. Tokura

Angaben zur Veröffentlichung / Publication details:

Hanasaki, N., K. Sano, Y. Onose, T. Ohtsuka, S. Iguchi, István Kézsmárki, S. Miyasaka, S. Onoda, N. Nagaosa, and Y. Tokura. 2008. "Anomalous Nernst effects in pyrochlore molybdates with spin chirality." *Physical Review Letters* 100 (10): 106601. <https://doi.org/10.1103/physrevlett.100.106601>.

Anomalous Nernst Effects in Pyrochlore Molybdates with Spin Chirality

N. Hanasaki,^{1,2} K. Sano,¹ Y. Onose,^{1,3} T. Ohtsuka,¹ S. Iguchi,¹ I. Kézsmárki,^{1,4} S. Miyasaka,^{1,5} S. Onoda,^{3,6}
N. Nagaosa,^{1,3,7} and Y. Tokura^{1,3,7}

¹*Department of Applied Physics, University of Tokyo, Tokyo 113-8656, Japan*

²*Department of Physics, Okayama University, Okayama 700-8530, Japan*

³*Spin Superstructure Project (SSS) and Multiferroics Project (MF), ERATO, Japan Science and Technology Agency, Tsukuba 305-8562, Japan*

⁴*Department of Physics, Budapest University of Technology and Economics, 1111 Budapest, Hungary*

⁵*Department of Physics, Osaka University, Toyonaka 560-0043, Japan*

⁶*RIKEN(The Institute of Physical and Chemical Research), Wako 351-0198, Japan*

⁷*Correlated Electron Research Center (CERC), National Institute of Advanced Industrial Science and Technology (AIST), Tsukuba 305-8562, Japan*

(Received 29 July 2007; published 12 March 2008)

The transverse thermoelectric (Nernst) effect on pyrochlore molybdates is investigated experimentally. In $\text{Nd}_2\text{Mo}_2\text{O}_7$ and $\text{Sm}_2\text{Mo}_2\text{O}_7$ with the spin chirality, the Nernst signal, which mostly arises from the transverse heat current (or equivalently the transverse Peltier coefficient α_{xy}), shows a low-temperature (20–30 K) positive extremum, whereas it is absent in $(\text{Gd}_{0.95}\text{Ca}_{0.05})_2\text{Mo}_2\text{O}_7$ with no single-spin anisotropy of the rare-earth ion and hence with no spin chirality. The correlation between the Hall conductivity σ_{xy} and α_{xy} in $\text{Nd}_2\text{Mo}_2\text{O}_7$ also indicates the spin chirality plays a significant role in the spontaneous (anomalous) Nernst effect.

DOI: [10.1103/PhysRevLett.100.106601](https://doi.org/10.1103/PhysRevLett.100.106601)

PACS numbers: 72.15.Jf, 71.27.+a, 75.25.+z, 75.50.Cc

The lattice-topological frustration in strongly correlated electron systems provides rich physics, such as large residual spin entropy in the ground state [1] and the emergence of complex spin structures. The latter occasionally arouses the cross-correlation effects between different physical quantities, as exemplified by a cycloid spin structure endowed with magnetic ferroelectricity [2,3]. Another typical example is the umbrellalike spin system with the scalar spin chirality, $\chi_{123} = \mathbf{S}_1 \cdot (\mathbf{S}_2 \times \mathbf{S}_3)$, which is proportional to the solid angle subtended by the neighboring spins \mathbf{S}_i ($i = 1-3$). The scalar spin chirality can drive the transverse charge transport, such as the anomalous Hall effect (AHE) [4]. The mutual tilting of the spins produces the Berry phase in the transfer interaction. Then, a hopping electron feels a fictitious magnetic field, which arouses the Hall conductivity σ_{xy} [4–8], as observed for pyrochlore molybdates with the umbrella spin structure [4,9–11]. One can expect the analogous spin-chirality effect also in the transverse thermoelectric effect (Nernst effect), where the thermal current replaces the charge current in the Hall effect [12]. Recently, Lee *et al.* reported the anomalous Nernst effect in the ferromagnetic metal spinels $\text{CuCr}_2\text{Se}_{4-x}\text{Br}_x$ [13]. They found that the transverse thermoelectric coefficient α_{xy} , as defined by the transport equation $J_i = \sigma_{ij}E_j + \alpha_{ij}(-\nabla T)_j$, is independent of the transport lifetime τ , which is consistent with the intrinsic Berry-phase scenario [5,7,12,14]. The ferromagnetic spinels $\text{CuCr}_2\text{Se}_{4-x}\text{Br}_x$ have a collinear magnetic structure, in which the Berry phase is produced via the spin-orbit interaction [5,6]. The Berry phase arising from the spin chirality is also expected to give rise to the transverse

thermoelectric phenomena, although this has never been investigated so far. In this Letter, we report on the thermoelectric effects in pyrochlore type $R_2\text{Mo}_2\text{O}_7$ ($R = \text{Nd}, \text{Sm}$, and $\text{Gd}_{0.95}\text{Ca}_{0.05}$), and discuss the contribution of the spin chirality to the anomalous Nernst effect.

For a large R -site radius r_R in the pyrochlore molybdate $R_2\text{Mo}_2\text{O}_7$, where the Mo-O-Mo angle is relatively large [15], the ferromagnetic state is stabilized with a nearly half-metallic character [16,17]. The comparative plot of magnetization and diagonal transport coefficients (resistivity and thermoelectric power) in Fig. 1 shows the itinerant ferromagnetism in the low-temperature phase of the three pyrochlore molybdates ($R = \text{Nd}, \text{Sm}$, and $\text{Gd}_{0.95}\text{Ca}_{0.05}$). For $R = \text{Nd}$, the Mo spins undergo a ferromagnetic transition at $T_c = 85$ K. The thick bar on the left ordinate in Fig. 1(a) corresponds to the saturated Mo spin moment ($\approx 1.4\mu_B/\text{Mo}$) deduced from the analysis of the neutron diffraction data [4,18]. Below ≈ 40 K, the $4f$ local spins on the Nd sites start to produce a net magnetic moment and then align antiparallel to the ferromagnetic $4d$ spins on the Mo sites due to the antiferromagnetic exchange coupling J_{fd} . This leads to the reduced total magnetization at low temperatures. The large spin-orbit interaction for Nd f electrons gives rise to the strong single-ion anisotropy, and hence the Nd^{3+} ($4f^3$) moments behave as Ising spins pointing toward or outward from the center of the Nd tetrahedron; these moments then form the two-in two-out umbrellalike spin structure. This non-coplanar spin structure on Nd sites is transmitted to the Mo spins via the $f-d$ spin exchange interaction J_{fd} [4,18]. The transmitted spin chirality on the Mo sites is responsible for the AHE at low

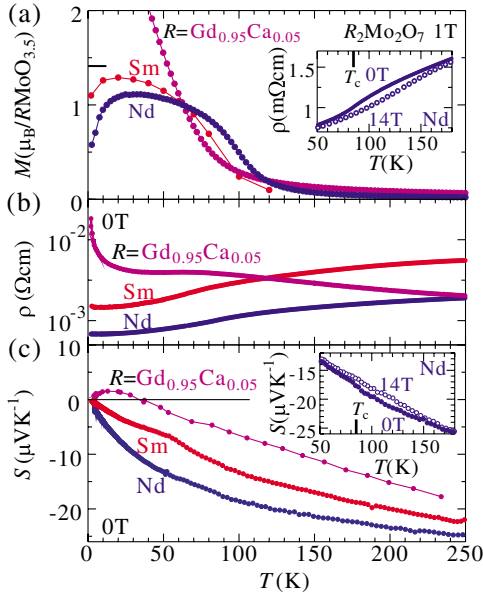


FIG. 1 (color online). Temperature dependence of (a) the magnetization M at $B = 1$ T and the longitudinal transport properties; (b) resistivity ρ and (c) Seebeck coefficient S at $B = 0$ T in $R_2\text{Mo}_2\text{O}_7$ ($R = \text{Nd}$, Sm , and $\text{Gd}_{0.95}\text{Ca}_{0.05}$). The horizontal thick bar on the left ordinate in (a) indicates the estimated value of the Mo spin moment from the neutron diffraction data [4,18]. The insets of (a) and (c) display ρ and S in $B = 0$ T and 14 T (closed and open circles) for $R = \text{Nd}$, respectively. The vertical thick bars in the insets indicate the ferromagnetic transition temperature (T_c) for $R = \text{Nd}$. The magnetic field was applied along the [111] direction.

temperatures [4,9,19,20]. (Note also some criticism [21] against this interpretation.) For $R = \text{Sm}$, as the Sm^{3+} moment is smaller than the Nd^{3+} one, the low-temperature reduction of the magnetization is small compared with $R = \text{Nd}$ [22]. On the other hand, for $R = \text{Gd}_{0.95}\text{Ca}_{0.05}$, the ferromagnetic exchange interaction J_{fd} enhances the magnetization at low temperatures. Since the Gd^{3+} ($4f^7$) spins without orbital angular momentum are Heisenberg-like, the $R = \text{Gd}_{0.95}\text{Ca}_{0.05}$ compound has a collinear Mo spin structure.

Single crystals were synthesized by the floating zone method in Ar gas, after the heat treatment of MoO_3 , Mo , R_2O_3 , and CaCO_3 (for $R = \text{Gd}_{0.95}\text{Ca}_{0.05}$). For $R = \text{Gd}$, we investigated a slightly Ca-doped sample ($R = \text{Gd}_{0.95}\text{Ca}_{0.05}$), since the hole doping via this procedure stabilizes the metallic state. The extrapolated zero-temperature conductivity has a finite positive value, suggesting the metallic ground state [23,24]. The Seebeck and the Nernst effects were measured with the use of the Quantum Design physical property measurement system. The temperature gradient along the sample (along the x axis) was generated by a RuO_2 resistance heater and was measured by Cernox thermometers attached to the sample edges. The corresponding thermal voltage built up across the sample (along the y axis) was measured by a nanovolt

preamplifier (Keithley 1801), while the magnetic-field strength was decreased from $B = \pm 14$ T. The Nernst signal $e_N (= [\partial V/\partial y]/[\partial T/\partial x])$ was obtained after the antisymmetrization procedure, such as $e_N = \{[V_y(B) - V_y(-B)]/2w\}/[\partial T/\partial x]$, to subtract the offset due to the inevitable asymmetry of the electrodes. Here, w denotes the sample width along the y axis.

Figure 1(c) displays the longitudinal thermoelectric (Seebeck) coefficient S in three pyrochlore molybdates $R_2\text{Mo}_2\text{O}_7$ ($R = \text{Nd}$, Sm , and $\text{Gd}_{0.95}\text{Ca}_{0.05}$), suggesting electronlike carriers in the metallic state. A considerable magnetic-field effect on the Seebeck coefficient was observed in $R = \text{Nd}$, as shown in the inset of Fig. 1(c). Namely, its absolute magnitude is decreased by the application of a magnetic field in $T = 70$ – 140 K, where the negative magnetoresistance [the inset of Fig. 1(a)] was simultaneously observed, owing to the reduction of the spin scattering. The decrease of $|S|$ is ascribed to the reduction of the spin entropy accompanied by the ferromagnetic state stabilized by the magnetic field. Such a magnetic-field effect on the Seebeck coefficient is independent of the field direction.

We show the transverse thermoelectric (Nernst) signal e_N in $\text{Nd}_2\text{Mo}_2\text{O}_7$ at various temperatures in Fig. 2. At higher temperatures, well above T_c , the Nernst signal e_N is nearly proportional to the magnetic-field strength. The deviation from linearity becomes clear below $T = 150$ K. At lower temperatures, the low-field Nernst signal is dramatically enhanced due to the onset of the spontaneous component, since the magnetic field aligns the ferromag-

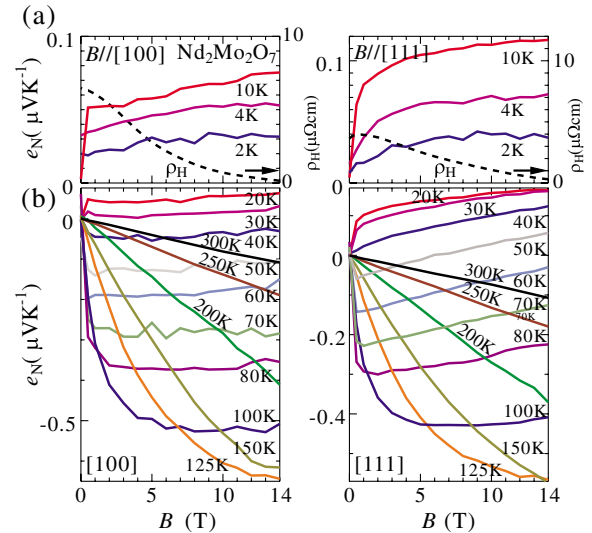


FIG. 2 (color online). Magnetic-field dependence of the transverse Nernst signal e_N for $\text{Nd}_2\text{Mo}_2\text{O}_7$, measured in the magnetic field along the [100] direction (left panel) and the [111] direction (right panel) below $T = 10$ K (a) and above $T = 20$ K (b). The broken curves of the upper panels indicate the magnetic-field dependence of the anomalous Hall resistivity ρ_H at 2 K, whose ordinates refer to the right-hand ones.

netic domains to the magnetic-field direction. Above $B = 1$ T, the Nernst signal increases gradually with the magnetic-field strength. Let us begin with analyzing the spontaneous component of the Nernst effect represented by the $e_N(B = 1 \text{ T})$ low-field value. A comparative plot for the temperature dependence of the Nernst coefficient and the Hall resistivity is given in Fig. 3 for each compound investigated. For $R = \text{Nd}$ and Sm , ρ_H and e_N have minima around the respective T_c , owing to the coupling with critical spin fluctuations through the spin-orbit interaction near the ferromagnetic transition, although the fluctuation of the spin chirality shifts the dip temperature in ρ_H up to ~ 110 K in $R = \text{Nd}$. The Hall resistivity ρ_H for $R = \text{Nd}$ and Sm is enhanced by the spin chirality at the lowest temperature [4], whereas it approaches zero for $R = \text{Gd}_{0.95}\text{Ca}_{0.05}$, with no spin chirality. In the former, the Nernst signal e_N changes its sign and reaches the maxima around $T = 20$ K, while in the latter it remains negative. Furthermore, its absolute value in the latter at low temperatures of $T < 20$ K is much smaller than in the former. This remarkable difference in e_N suggests that the spin chirality contributes to the low-temperature positive component of e_N , as observed for $R = \text{Nd}$ and Sm .

Let us examine the transverse Peltier coefficient α_{xy} , which is expressed as $\alpha_{xy} = -[e_N - (\rho_{yx}/\rho_{xx})S]/\rho_{xx}$ [13]. We used the experimental value of the resistivity ρ_{xx} , the Seebeck coefficient S , and the Hall resistivity ρ_{yx} . The α_{xy} is an essential quantity for the thermal transport phenomena, since the α_{xy} is theoretically expected to be expressed by the Berry phase [12,14]. The magnitude of

α_{xy} is much larger than that of $\rho_{yx}S/\rho_{xx}^2$, indicating that the Nernst signal e_N mostly arises from the transverse heat current, as described by α_{xy} . The temperature dependence of the Peltier coefficient α_{xy} for $\text{Nd}_2\text{Mo}_2\text{O}_7$ was investigated in both the low-field and high-field regions ($B = 1$ and 14 T, respectively), as shown in Fig. 4(c). The low-field value reaches a maximum at $T \approx 85$ K, which is attributed to the ferromagnetic spin fluctuation near T_c [25]. The similar enhancement of α_{xy} around T_c is ubiquitously observed in itinerant ferromagnets [13,26]. Towards lower temperatures, the α_{xy} changes its sign at $T = 40$ –60 K, and then approaches zero following a nearly linear temperature dependence for the both magnetic-field directions along [100] and [111]. In the high magnetic field ($B = 14$ T), the peak temperature of α_{xy} increases up to $T \approx 130$ K, since the magnetic field stabilizes the ferromagnetic state up to higher temperatures, as indicated by the magnetization and the Seebeck effect at $B = 14$ T in

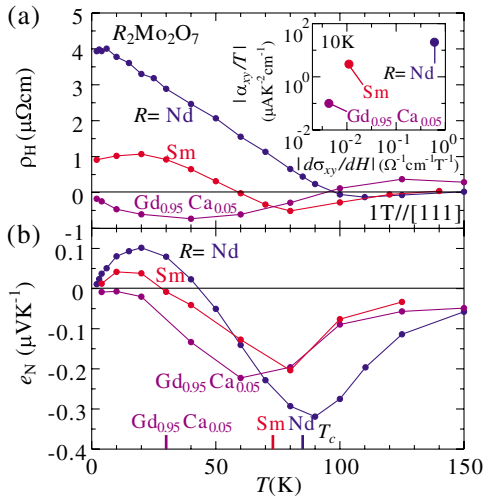


FIG. 3 (color online). R -site dependence of (a) the Hall resistivity ρ_H and (b) the Nernst signal e_N in $R_2\text{Mo}_2\text{O}_7$ ($R = \text{Nd}$, Sm , and $\text{Gd}_{0.95}\text{Ca}_{0.05}$). Magnetic field of $B = 1$ T was applied along the [111] direction. The vertical thick bars on the bottom abscissa indicate the ferromagnetic transition temperatures, $T_c = 85$ K, 73 K, and 30 K in $R = \text{Nd}$, Sm , and $\text{Gd}_{0.95}\text{Ca}_{0.05}$, respectively. Inset: $|\alpha_{xy}/T|$ as a function of $|\partial\sigma_{xy}/\partial H|$ at 10 K on a logarithmic scale.

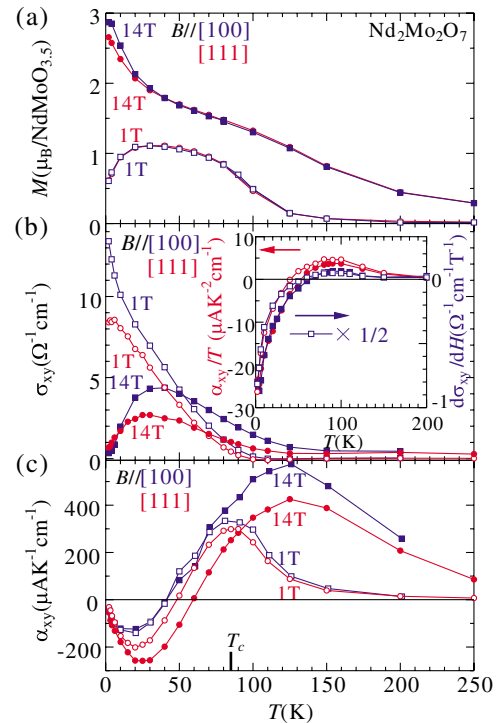


FIG. 4 (color online). (a) The magnetization M , (b) the Hall conductivity σ_{xy} , and (c) the transverse Peltier coefficient α_{xy} for the applied magnetic field of $B = 1$ T (open squares and circles) and $B = 14$ T (closed squares and circles) along the [100] (blue online) and [111] (red) directions in $\text{Nd}_2\text{Mo}_2\text{O}_7$, respectively. The vertical thick bar on the bottom abscissa indicates the ferromagnetic transition temperature ($T_c = 85$ K). Inset: Temperature dependence of α_{xy}/T [(red) open and closed circles] and $\partial\sigma_{xy}/\partial H$ [(blue) open and closed squares] for the applied magnetic field of 5 T along the [100] and [111] directions, respectively. The value of $\partial\sigma_{xy}/\partial H$ at 5 T was obtained by the differential procedure as $[\sigma_{xy}(5 \text{ T}) - \sigma_{xy}(4 \text{ T})]/1 \text{ T}$.

Fig. 1(c) and 4(a), respectively. The anisotropy of α_{xy} (14 T) with respect to the magnetic-field direction becomes clear below $T = 150$ K. In the same temperature range, the anisotropy of the σ_{xy} (14 T) was observed as well, which can be ascribed to the spin-chirality contribution; the fluctuation of the spin chirality contributes to the σ_{xy} , even with a small uniform magnetization [20]. Thus, the simultaneous emergence of anisotropy in σ_{xy} and α_{xy} is suggestive of the contribution of the spin chirality to α_{xy} as well.

The magnetic-field dependence of the AHE at $T = 2$ K is shown by the dashed line in Fig. 2(a). The decrease of the Hall resistivity ρ_H by the application of a high magnetic field is attributed to the reduction of the amplitude of the spin chirality, since the magnetic field aligns the Mo moments along the field direction [4,9,19]. In other words, the magnetic-field dependence of the Hall resistivity, as represented by the quantity $\partial\sigma_{xy}/\partial H$, indicates the spin-chirality contribution in σ_{xy} , since the normal component of the Hall conductivity is negligibly small compared with the anomalous one. The inset of Fig. 4(b) depicts α_{xy}/T in comparison with $\partial\sigma_{xy}/\partial H$ at $B = 5$ T, where the magnitude of $\partial\sigma_{xy}/\partial H$ reaches nearly a maximum value and the magnetic-field-induced change of the spin chirality is expected to be the largest. Both quantities show nearly identical temperature dependence, ensuring the contribution of the spin chirality to α_{xy} . This scaling behavior is reminiscent of the Mott rule, $\alpha_{ij}/T = (\pi^2 k_B^2 / 3e) [\partial\sigma_{ij}(\epsilon) / \partial\epsilon]_{\epsilon=\mu}$, where k_B , e , and μ are the Boltzmann's constant, the electron charge, and the chemical potential, respectively [12,14]. The magnetic field lowers the energy level of the majority spin band and raises that of the minority spin band, leading to the shift of the chemical potential level μ , when the density of states is different for different spins. Thus, the magnetic-field derivative can be considered as the energy derivative in each spin band with the opposite signs. Since the Mo spins are almost fully polarized, we obtain $\partial\sigma_{xy}/\partial H \approx g\mu_B ([\partial\sigma_{xy}^{\text{maj}} / \partial\epsilon]_{\epsilon=\mu} - [\partial\sigma_{xy}^{\text{min}} / \partial\epsilon]_{\epsilon=\mu})$. The majority spin band dominantly contributes to σ_{xy} . Thus, one finds $\alpha_{xy}/T \approx (\pi^2 k_B^2 / 3e)(1/g\mu_B) [\partial\sigma_{xy}^{\text{maj}} / \partial H]$, using the Mott rule. From the scaling analysis shown in the inset of Fig. 4(b), the ratio of α_{xy}/T to $\partial\sigma_{xy}/\partial H$ is estimated as 3×10^{-5} V T/K², which is on the order of $(\pi^2 k_B^2 / 3e) \times (1/g\mu_B) \sim 1 \times 10^{-4}$ V T/K². The suppression in the experimental value may stem from the reduced spin chirality under the magnetic field ($B = 5$ T). According to the theoretical study [7,26], in the fairly resistive region of $\sigma_{xx} \sim 10^3 \Omega^{-1} \text{cm}^{-1}$ as in Nd₂Mo₂O₇, the skew-scattering effect and the side-jump scattering effect are negligibly small, as compared with the intrinsic Berry-phase effect. To confirm the correlation between $|\alpha_{xy}/T|$ and $|\partial\sigma_{xy}/\partial H|$ in different compounds, the inset of

Fig. 3(a) depicts $|\alpha_{xy}/T|$ as a function of $|\partial\sigma_{xy}/\partial H|$ at 10 K for $R = \text{Nd}$, Sm , and $\text{Gd}_{0.95}\text{Ca}_{0.05}$; in common to all the compounds $|\alpha_{xy}/T|$ increases with $|\partial\sigma_{xy}/\partial H|$.

In conclusion, the observed Nernst signal e_N arises mostly from the transverse Peltier coefficient α_{xy} . In $R = \text{Nd}$, possessing the spin chirality, the α_{xy} shows the positive maximum around the ferromagnetic transition, then the negative maximum due to the spin chirality. The negative values of α_{xy} in $R = \text{Nd}$ and Sm at low temperatures ($T < 40$ K) are in sharp contrast to the positive value of α_{xy} in the ferromagnetic phase of $R = \text{Gd}_{0.95}\text{Ca}_{0.05}$ without spin chirality. In accord with the anticipation from the Mott rule, a close correlation is observed between α_{xy}/T and $\partial\sigma_{xy}/\partial H$, the latter of which has been assigned to the hallmark of the spin chirality, suggesting an important role of the spin chirality also in the thermal transport phenomena. On the basis of these observations, the contribution of the spin chirality has been identified in the anomalous Nernst effect.

The authors are grateful to A. Asamitsu, T. Miyasato and Y. Taguchi for enlightening discussions. This work was partly supported by Grant-in-Aids for Scientific Research (No. 15104006, No. 16076205, No. 17340104, and No. 19014015) and on Priority Areas ‘‘Novel States of Matter Induced by Frustration’’ (No. 19052003) and by the Hungarian OTKA No. F61413.

-
- [1] S. T. Bramwell and M. J. P. Gingras, *Science* **294**, 1495 (2001).
 - [2] T. Kimura *et al.*, *Nature (London)* **426**, 55 (2003).
 - [3] H. Katsura *et al.*, *Phys. Rev. Lett.* **95**, 057205 (2005).
 - [4] Y. Taguchi *et al.*, *Science* **291**, 2573 (2001).
 - [5] Z. Fang *et al.*, *Science* **302**, 92 (2003).
 - [6] W. L. Lee *et al.*, *Science* **303**, 1647 (2004).
 - [7] S. Onoda *et al.*, *Phys. Rev. Lett.* **97**, 126602 (2006).
 - [8] G. Sundaram and Q. Niu, *Phys. Rev. B* **59**, 14915 (1999).
 - [9] Y. Taguchi *et al.*, *Phys. Rev. Lett.* **90**, 257202 (2003).
 - [10] T. Kageyama *et al.*, *J. Phys. Soc. Jpn.* **70**, 3006 (2001).
 - [11] Y. Machida *et al.*, *Phys. Rev. Lett.* **98**, 057203 (2007).
 - [12] F. D. M. Haldane, *Phys. Rev. Lett.* **93**, 206602 (2004).
 - [13] W. L. Lee *et al.*, *Phys. Rev. Lett.* **93**, 226601 (2004).
 - [14] D. Xiao *et al.*, *Phys. Rev. Lett.* **97**, 026603 (2006).
 - [15] Y. Moritomo *et al.*, *Phys. Rev. B* **63**, 144425 (2001).
 - [16] T. Katsufuji *et al.*, *Phys. Rev. Lett.* **84**, 1998 (2000).
 - [17] M. W. Kim *et al.*, *Phys. Rev. Lett.* **92**, 027202 (2004).
 - [18] Y. Yasui *et al.*, *J. Phys. Soc. Jpn.* **72**, 865 (2003).
 - [19] S. Iguchi *et al.*, *Phys. Rev. B* **69**, 220401 (2004).
 - [20] S. Onoda and N. Nagaosa, *Phys. Rev. Lett.* **90**, 196602 (2003).
 - [21] Y. Yasui *et al.*, *J. Phys. Soc. Jpn.* **75**, 084711 (2006).
 - [22] Y. Taguchi and Y. Tokura, *Europhys. Lett.* **54**, 401 (2001).
 - [23] I. Kézsmárki *et al.*, *Phys. Rev. B* **73**, 125122 (2006).
 - [24] N. Hanasaki *et al.*, *Phys. Rev. Lett.* **96**, 116403 (2006).
 - [25] Y. Lyanda-Geller *et al.*, *Phys. Rev. B* **63**, 184426 (2001).
 - [26] T. Miyasato *et al.*, *Phys. Rev. Lett.* **99**, 086602 (2007).
 - [27] I. V. Solovyev, *Phys. Rev. B* **67**, 174406 (2003).